LIGO-T970240-00-D

HYTEC-TN-LIGO-17
06/05/97

Low Frequency Damping Measurement Setup and First Results

Eric Ponslet
June 5, 1997

Abstract

A specialized setup for measuring low frequency (1 Hz range) stiffnesses and loss factors of LIGO springs is described. First experimental results on coil spring and leaf spring prototypes are also presented.

HYTEC Inc.
110 Eastgate Dr., Ste 100
Los Alamos, NM 87544
(505) 661-3000 / Fax (505) 662-5179

LIGO PROJECT

Table of Contents

1. Experimental Setup

1.1 Motivation

The springs static load capacity (100 lbf) and stiffnesses dictate a lower bound on natural frequencies achievable with a single degree of freedom, axial spring mass system, of about 4 Hz (see spring test report[1]). Unfortunately, the critical frequency for spring loss factor is that of the first isolation stack resonance, or about 1.3 Hz, where large quality factors (Q = inverse of loss factor η) make LSC control system design difficult. Because spring loss factors are strongly frequency dependent, it is therefore critical to obtain reliable experimental measurements of the loss factors/Q's and stiffnesses in axial and shear directions of the springs considered for the LIGO isolation stacks. Those measured loss factors and stiffnesses can then be incorporated into SIS simulations to obtain good estimates of the lowest natural frequencies, mode shapes, and quality factors of the stacks.

1.2 Description of Apparatus

The apparatus uses the rotational inertia of a large, symmetric, horizontal pendulum to produce low frequency resonance of the single degree of freedom system formed by the pendulum and a spring. Variable amounts of mass can be attached at the tips of the beam to vary the inertia of the pendulum and the frequency of the measurement. Instrumentation measures the free decay of the pendulum oscillation and post-processing provides loss factors and stiffnesses of the springs.

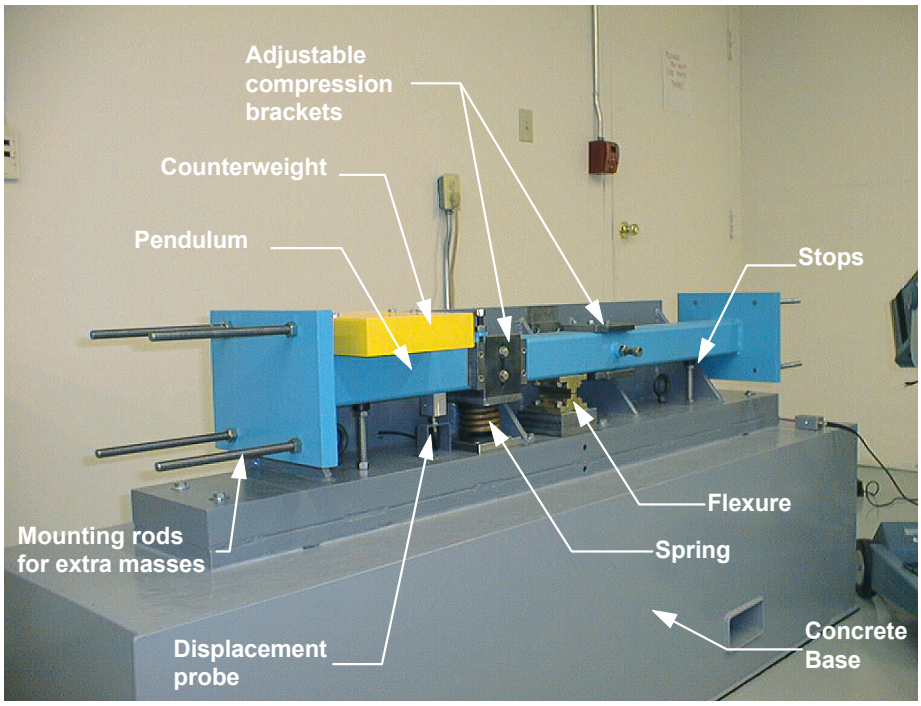

Figure 1: Low frequency spring measurement setup.

The setup is shown in Fig. 1. The pendulum beam (in blue) is made of a 3×3×1/4" steel box beam, with 1" plates welded at the ends to support extra tip masses. The beam is supported at its center on a brass flexure, 3" deep, with a .031" neck. Two steel and rubber stops limit the swing of the pendulum to protect the flexure. The whole system is build on a solid 3" steel base plate (dark grey). That plate is in turn anchored and grouted to a 6×1.5×1.5 ft solid concrete block (light grey). That block is resting on a ¼" felt layer on the building's concrete slab.

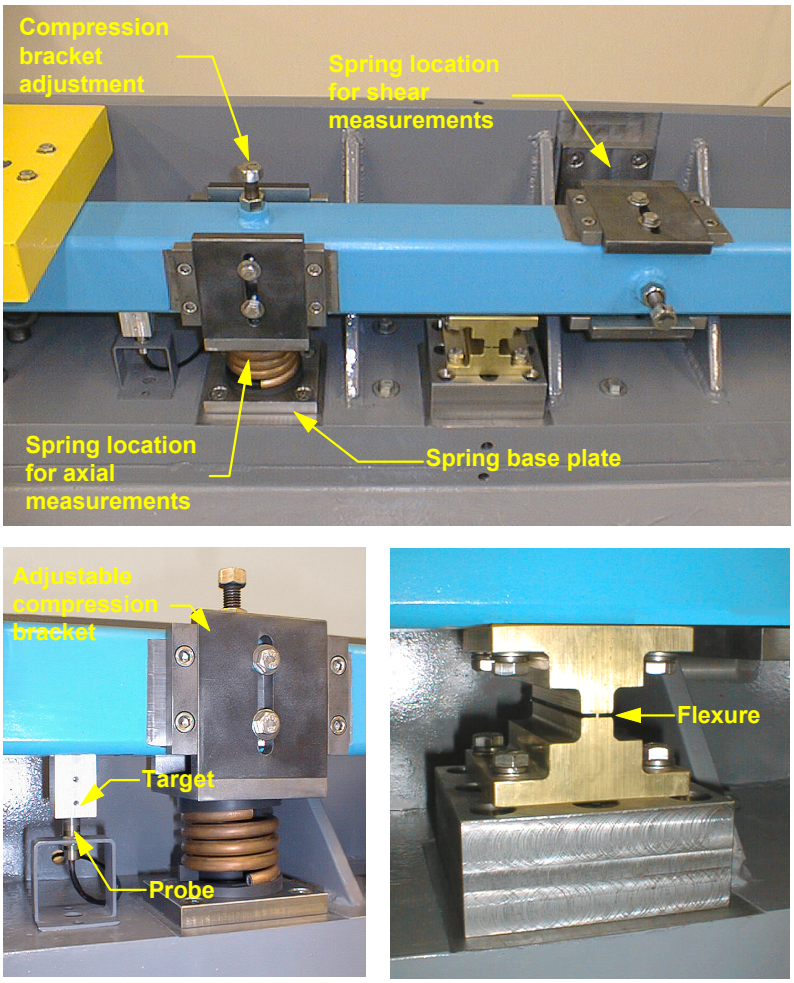

Figure 2: Closeups on the low frequency spring measurement setup, showing the axial and shear spring measurement locations, the displacement probe, and the flexure.

A non-contact inductive displacement probe is mounted on the base on one side of the flexure. The probe measures the displacement of an aluminum target (Fig. 2, lower left) bonded to the main beam. The spring can be mounted at one of two locations, depending on whether axial or shear properties will be measured (Fig. 2, upper). Each of those locations features a removable spring base plate bolted to the system's steel base. The design of that base plate is different for different types of springs (leaf or coil). Each location also features an adjustable "U" bracket attached to the pendulum beam. That

bracket allows for adjustment of the spring static preload. When the spring is mounted in the axial location (as in Figs. 1 and 2), a counterweight (Fig.1, yellow) is bolted on top of the pendulum beam to provide the axial preload on the spring, and the "U" bracket is used to adjust the pendulum initial position. When the spring is mounted in the shear position, the counterweight is removed, the "U" bracket adjusts the preload, and the flexure resists the resulting twisting moment.

The complete moving part of the pendulum weighs about 47 kg with no counterweight or added tip masses. This weight can be increased to a maximum of 170 kg by adding tip masses weighing 10.2 kg each. The corresponding variation of rotational mass moment of inertia around the flexure is from 11.6 kg.m^2 to 77.1 kg.m^2. This in turn provides adjustability of the measurement frequency by a factor 2.5, with constant static preload on the spring. For typical metal springs used in the LIGO project, the measurement frequency band is about 0.7 Hz to 1.8 Hz.

1.3 Data Extraction

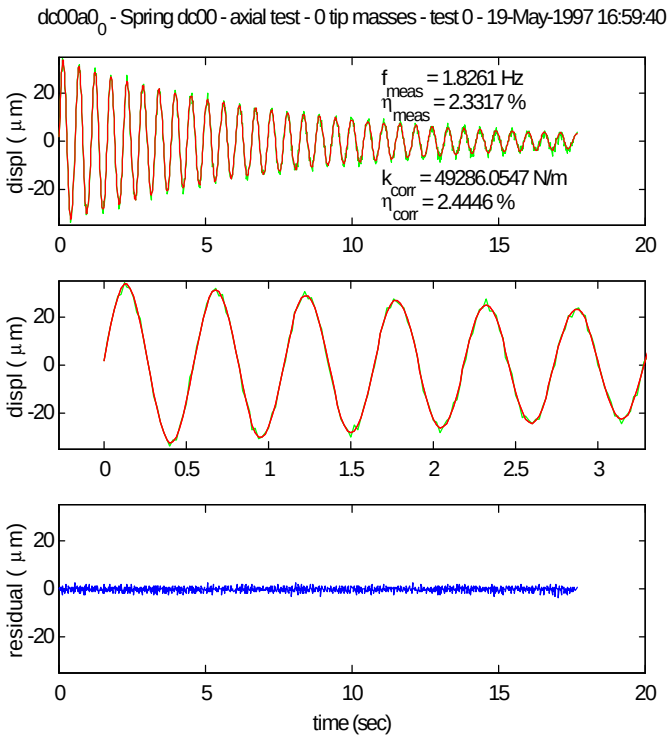

Figure 3: Typical experimental data and fit. top chart shows raw signal (green) and fitted decaying sinusoid (red); middle chart shows 5 first periods on enlarged time scale; bottom chart is residual noise (=difference between signal and fitted sinusoid).

Measurements are taken by exciting the pendulum by hand and recording probe signal versus time during free decay. The data is acquired such that the initial peak to peak spring deflection amplitude is consistently equal to about 65 μm in the axial setup and 48 μm in the shear setup. That data, together with calculated mass properties of the setup, provides a measure of the total rotational stiffness around the hinge line and total damping in the system, represented by the complex stiffness κ_{meas}. Stiffness and damping

are extracted using least square fit of a exponentially decaying sinusoid to the probe's signal. A typical signal and fit result is shown in Fig. 3. Note how the fit technique makes the measurement immune to random noise.

The top chart in Fig. 3 also lists frequency and loss factor of fitted sinusoid (f_{meas}, η_{meas}) as well as corrected values of spring stiffness and loss factor (k_{corr}, η_{corr}). Those corrected values are obtained after compensating for other sources of stiffness in the system, beside the spring itself: the bending stiffness of the flexure k_{flex}, and a negative stiffness effect due to gravity and the position of the pendulum center of mass above the hinge line. The last effect is easily calculated for each configuration of tip masses as

$$k_g = -Mgd,$$

where M is the total mass of the pendulum, g the acceleration of gravity, and d the vertical offset between the flexure hinge line and the pendulum center of mass. This effect k_g, ranges from about -32 Nm/rad with no added mass to about -116 Nm/rad with maximum added mass.

The flexure rotational stiffness was measured trough free decay of the pendulum/flexure system, without spring. Results with different amounts of tip mass gave very consistent values of that stiffness k_{flex}, averaging 157.5 Nm/rad.

The rotational stiffness effect from the spring is $k_{spring} = k_{spring} d_{spring}^2$, where k_{spring} is the axial or shear stiffness of the spring and d_{spring} the distance from hinge line to spring centerline. That effect κ_{spring} ranges from about 3650 Nm/rad to 9200 Nm/rad depending on spring type and and its location in the shear or axial configuration .

The measured rotational stiffness k_{meas} (complex number) is corrected by substracting the flexure and gravity effects to obtain the axial or shear complex stiffness of the spring as

$$k_{spring} = \frac{k_{meas} - k_{flex} - k_g}{d_{spring}^2}.$$

The spring stiffness k_{corr} and loss factor η_{corr} are then obtained as the real part and the ratio of imaginary to real part of k_{spring}, respectively. Note that the stiffness correction above represents only a few percent of the spring stiffness and loss factor.

Finally, tests were also conducted to evaluate any parasitic loss in the system: free decay measurements were performed with an off-the-shelf, undamped steel coil die spring. Measured loss factors were less than 0.1 %.

2. Experimental Results

2.1 A Note about Temperature Effects in the Coil Springs

All test results presented in this report were obtained in an uncontrolled environment, where - even though special care was taken to avoid them - temperature variations due to HVAC cycling, time of day, human presence, etc. can be of the order of 1 to 2 ºC over the few hours required for a full series of tests. Because the damping in the springs is entirely due to viscoelastic effects (either in the spring itself or the rubber seat)

and viscoelastic materials are very sensitive to temperature, some degree of pollution of the results by temperature effects should be expected.

To get some measure of the possible magnitude of these effects, we have extended the the closed form analytical expressions for coil spring damping (see [2]) to incorporate the effects of temperature on shear modulus and loss factor of the damping material. This analysis shows that temperature effects on loss factor of the composite coil spring alone (without rubber seats) can be as large as $\partial h/\partial T \approx 8$ %/ºC (relative variation in loss factor per degree change in temperature).

To summarize, with laboratory temperature fluctuations of the order of +/- 1ºC, and temperature sensitivity of the loss factor of the order of 8 %/ºC, we can expect scatter and/or drift in observed damping of up to 8% due to temperature effects only

2.2 Amplitude Effects - Damped Coil Pre-Prototype DC00

Tests were conducted to detect any amplitude dependence in the spring loss factor. Prototype spring DC00 was installed in the setup and the pendulum was loaded with maximum tip masses (61 kg at each tip). Free decay data was then acquired in axial and shear directions, and for different values of the peak-to-peak spring deflection amplitude. The results are shown in Fig. 4.

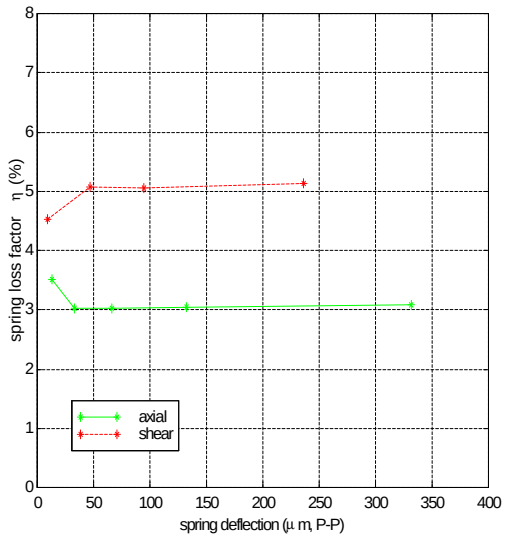

Figure 4: Spring loss factor versus spring deflection amplitude measured on DC00, on Viton seats, at 0.765 Hz in axial direction and 0.658 Hz in shear direction. Temperature extremes were 21°C and 22.5°C.

The figure shows that measured loss factor is remarkably insensitive to deflection amplitude for amplitudes greater than 50μm (the very slight slope in the curves could be due to amplitude effects OR to a temperature change of the order of a few tenth of a degree C). At smaller amplitude, the results show up to 20% deviation in measured loss factor. However, at such small amplitude, electronic noise from the displacement probe becomes significant: the signal to noise ratio in those measurements drops to less than 4. Also note that the shear and axial loss factors show opposite effects while a physical amplitude dependence effect would be expected in the same direction for both shear and

axial losses. These observations lead us to suspect that measurement noise - and not an actual amplitude dependence - is responsible for the deviations in measured values at very low deflections.

2.3 Coil Pre-Prototype DC00 on Epoxy Seats

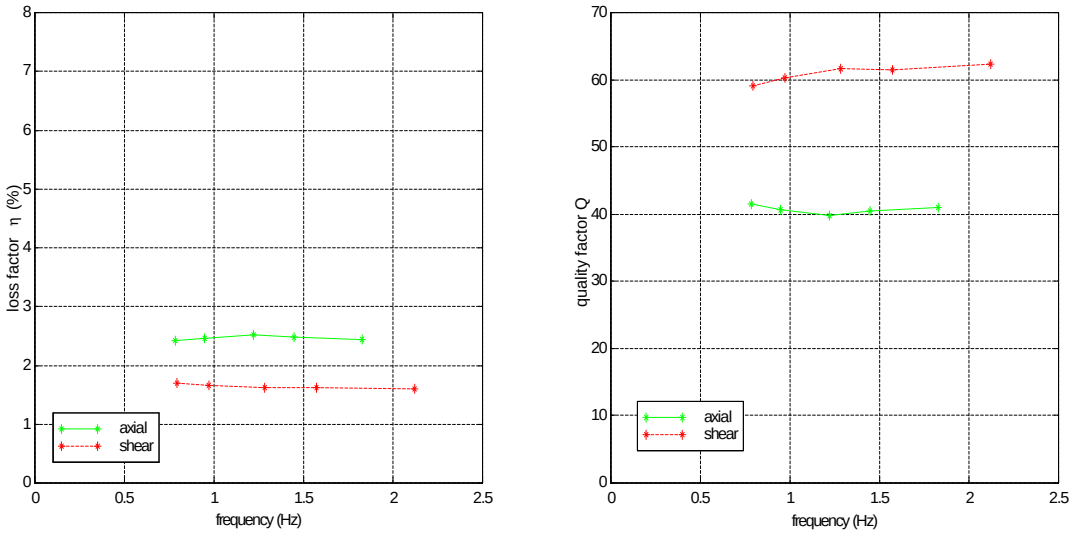

Figure 5: Loss factor and quality factor in axial and shear directions of DC00 on epoxy seats as a function of frequency. Temperature extremes were about 21°C and 21.5°C.

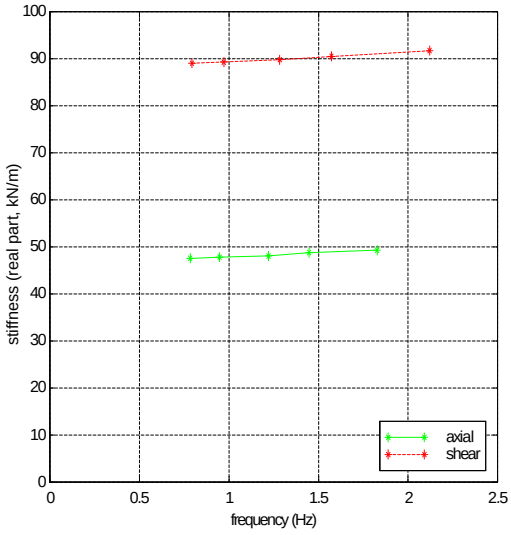

Figure 6: stiffnesses in axial and shear directions of DC00 on epoxy seats as a function of frequency. Temperature extremes were about 21°C and 21.5°C.

2.4 Coil Pre-Prototype DC00 on Fluorel Seats

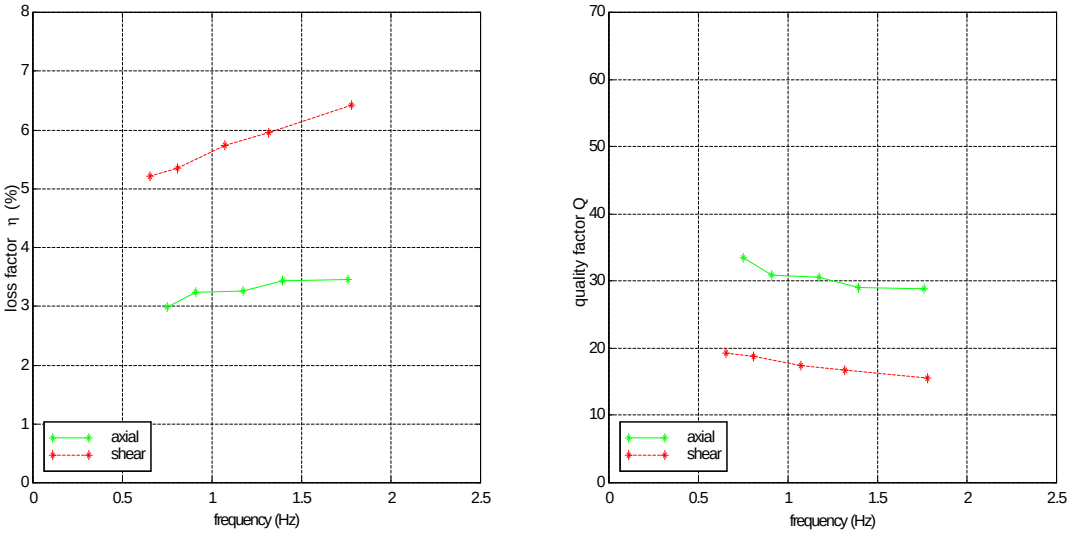

Figure 7: Loss factor and quality factor in axial and shear directions of DC00 on Fluorel seats as a function of frequency. Temperature extremes were 20.5°C and 22°C.

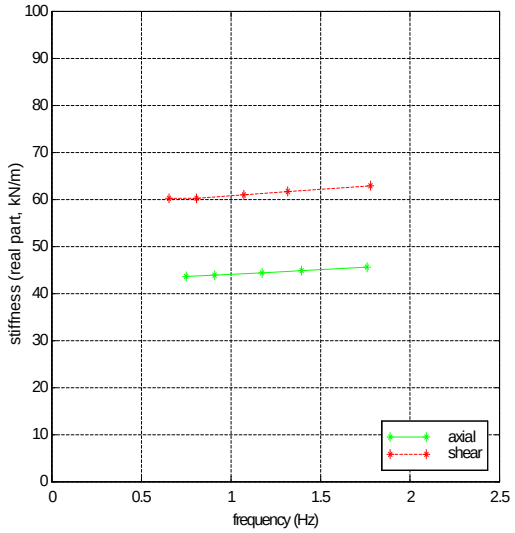

Figure 8:Stiffnesses in axial and shear directions of DC00 on Fluorel seats as a function of frequency. Temperature extremes were 20.5°C and 22°C.

2.5 Damped Coil Prototypes DC01, DC02 DC03 on Fluorel Seats

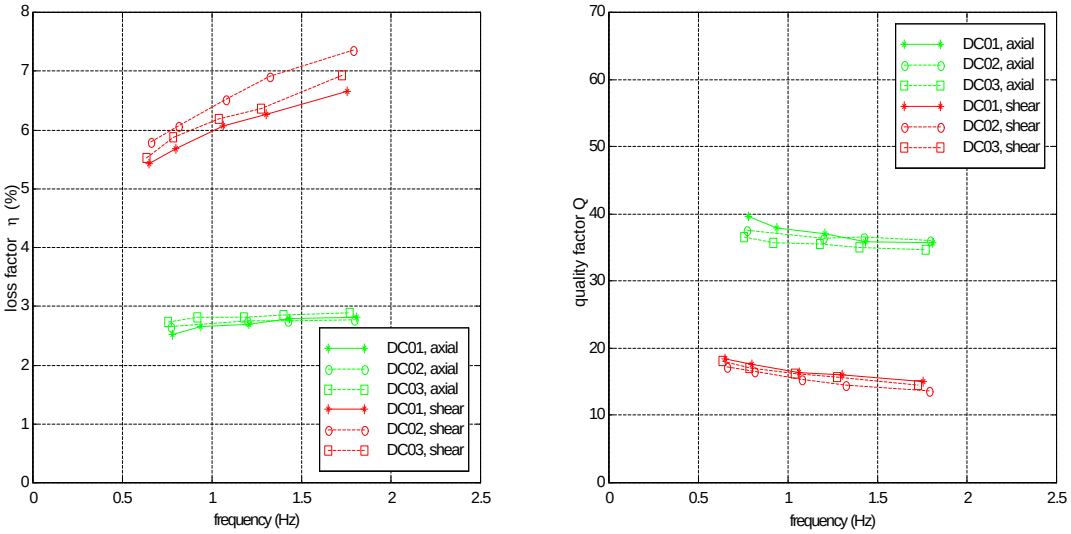

Figure 9: Loss factor and quality factor in axial and shear directions of DC01, DC02, and DC03 on Fluorel seats as a function of frequency. Temperature extremes were 21.1°C and 22.1°C.

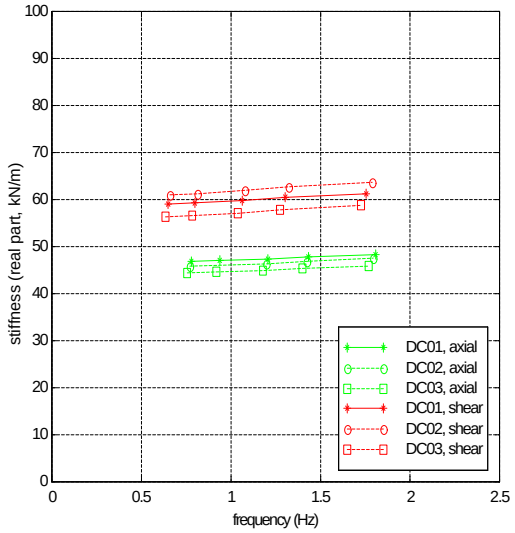

Figure 10: Stiffnesses in axial and shear directions of DC00 on Fluorel seats as a function of frequency. Temperature extremes were 21.1°C and 22.1°C.

2.6 Stiffness and Loss VS Frequency - Leaf Spring Prototype LF04

the leaf spring has two clearly distinct shear directions denoted 'S' and 'C' and illustrated in Fig. 11.

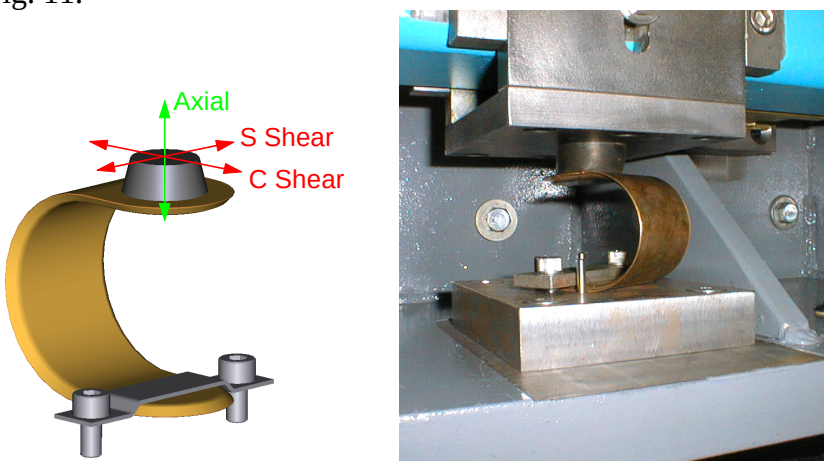

Figure 11: Leaf spring: definition of "S" and "C" shear directions (left) and top view of leaf spring in C shear test position (right).

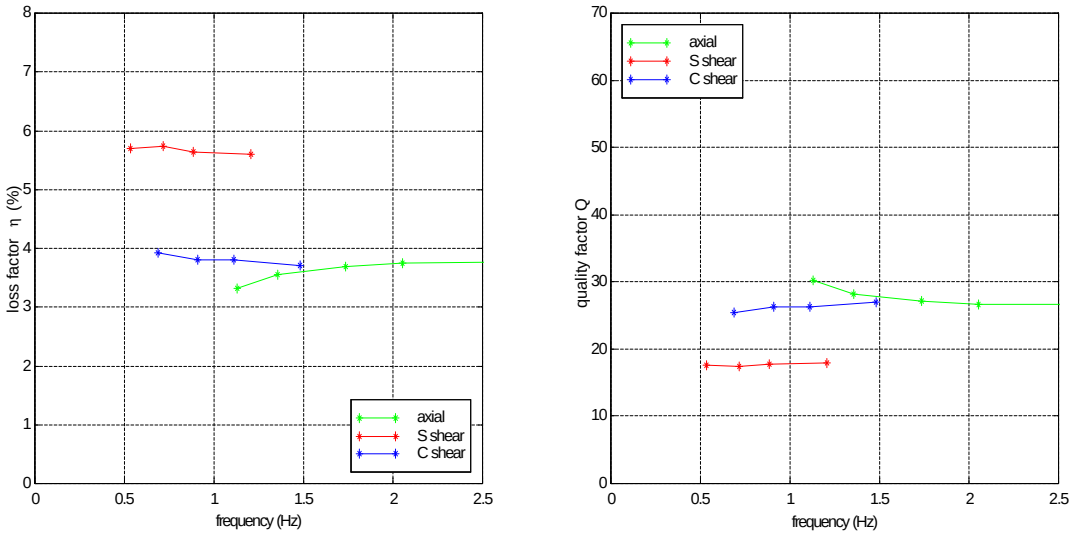

Figure 12: Loss factor and quality factor in axial and both "S" and "C" shear directions of leaf spring LF04 as a function of frequency. Temperature extremes were 22.6°C and 22.9°C.

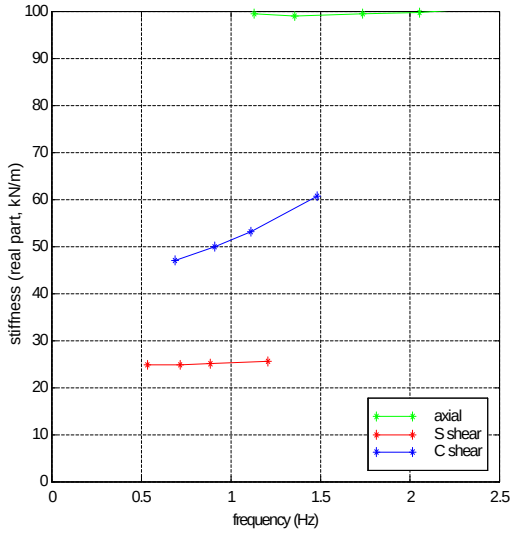

Figure 13: Stiffnesses in axial and both "S" and "C" shear directions of leaf spring LF04 as a function of frequency. Temperature extremes were 22.6°C and 22.9°C.

2.7 Summary - Spring Q's at First Stack Resonance

To summarize the above results, table 1 lists approximate values of spring Q's in axial and shear directions, estimated at the frequencies of the first resonance of the corresponding BSC stack. Note that those frequencies are based on stack models using pre-test spring properties, so that they only are approximations. Note also however that in all results shown in the previous sections measured Q's do not vary rapidly with frequency.

The Q of the first mode of the stack should be expected to fall somewhere between the shear and axial values for the spring.

Spring(s)	Lowest stack resonance frequency (estimate)	Q_{axial}	Q_{shear}
Damped coil on stiff seat (DC00)	1.28	40	62
Damped coil on Fluorel seat			
- DC00	1.28	29	17
- DC01, 02, and 03 (mean)	1.28	36	16
Leaf spring with rubber tip	1.37	28	27 (C), 18(S)

Table 1: summary of measured spring Q's at expected first stack resonance frequency.

2.8 Undamped Tubular Coil HC00 on Fluorel Seats

Spring HC01 is one of 3 hollow tubular springs without any damping treatment or core that were produced to allow measurements of loss factors due to fluorel seats only (since the springs do not contribute any damping). Those springs were produced from the same phosphor bronze tubing, first swaged to reduce its diameter then coiled to the same geometry as the damped springs.

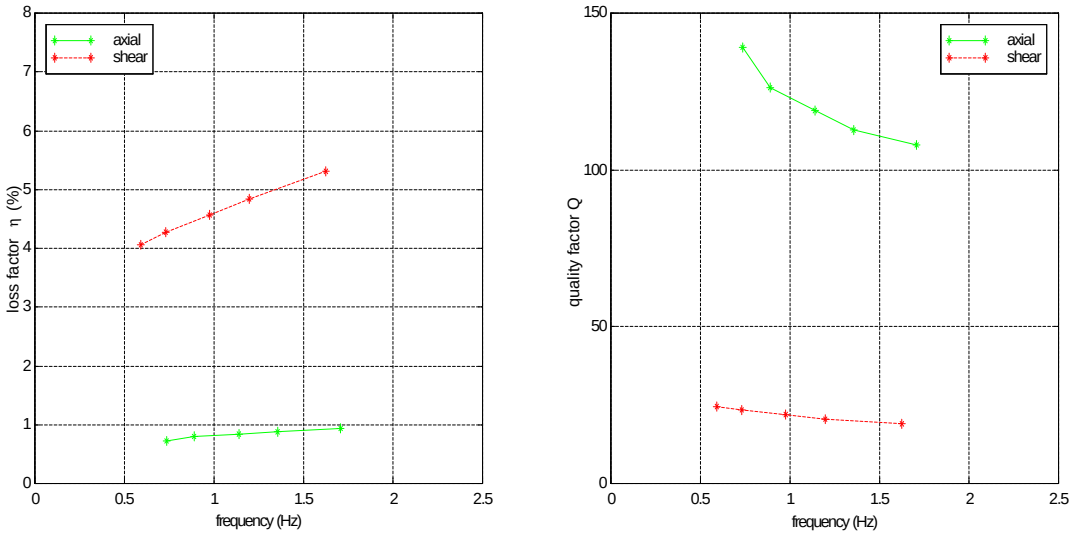

Figure 14: Loss factor and quality factor in axial and shear directions of HC01 on Fluorel seats as a function of frequency. Temperature extremes were 21.2°C and 21.5°C.

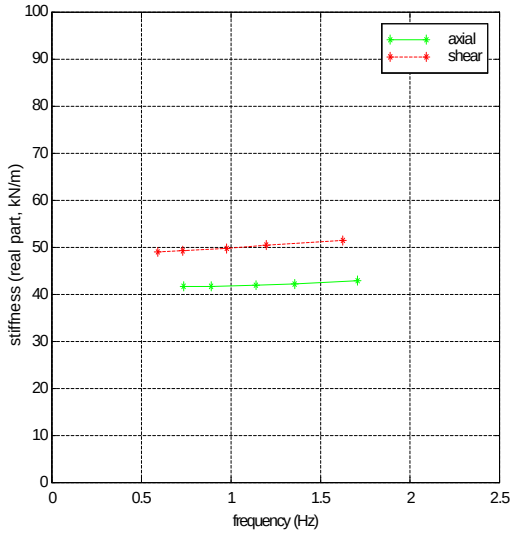

Figure 15:Stiffnesses in axial and shear directions of HC01 on Fluorel seats as a function of frequency. Temperature extremes were 21.2°C and 21.5°C.

3. References

1. E. Ponslet, *LIGO Coil Spring - Test Report*, HYTEC Inc., Los Alamos, NM, document HYTEC-TN-LIGO-14, February 1997.
2. E. Ponslet, *Design of Vacuum Compatible Damped Metal Springs for Passive Isolation of The LIGO Detectors*, HYTEC Inc., Los Alamos, NM, document HYTEC-TN-LIGO-04a (revision *a*), January 1997.

Note 1, Linda Turner, 09/03/99 01:24:55 PM
LIGO-T970240-00-D